Improved attitude stabilisation system augmented sounding rocket design, integration, verification & launch ⋆

Alexandra Posta * **Alexandre Monk** * **Antoine Durollet** ** **Oliver Martin** * **Sam Bruton** * **Jongrae Kim** **

* *Mechatronics & Robotics, University of Leeds, Leeds, LS2 9JT UK (e-mail: el19a2p,el19a2m,,el19ol,el19sab@leeds.ac.uk).*
** *School of Mechanical Engineering, University of Leeds, Leeds, LS2 9JT UK (e-mail: mn20a2d,menjkim@leeds.ac.uk).*

Abstract: A common barrier to maximising the altitude of a sounding rocket is the attitude deviation from the vertical flight induced by wind, known as weather cocking. An active stabilisation with canards, which was first proposed and implemented in the previous academic year (2022-23), is significantly improved as follows: a compact flight computer, a robust canard mechanical system, the linear quadratic regulator gain tuned and a new telemetry with extended data monitoring/analysis. The verification process, which includes the flight mode detection, the wind tunnel experiment, the telemetry test and the attitude estimation test, has been performed. A successful launch in April 2024 shows the effectiveness of the integrated attitude control system and the ground data supporting system.

Keywords: Sounding rocket, weather cocking, canard, attitude control, system integration

1. INTRODUCTION

Sounding rockets, platforms used for suborbital testing and atmospheric studies (Seibert and Battrick, 2006), often encounter trajectory deviations due to wind and other external disturbances (Candidato et al., 2014). These disturbances can lead to unwanted dispersion and diminished peak altitudes, i.e., the apogee. Whilst the flight angle of a rocket can be controlled to some degree through passive stability, a common obstacle to vertical flight is the tilting of a rocket by the wind, an effect known as weather cocking (Box et al., 2011). To counteract weather cocking and allow more vertical trajectories, different active stability systems have been developed. By incorporating active vertical controllers, the trajectory of the rocket can be corrected, thus generating a safer and more reliable flight.

The most common active control systems being a gimbaled-engine exhausts which permit thrust vectoring (Hervas and Reyhanoglu, 2014). Another method is using control surfaces on the passive fins, which work in the same ways as the ones on aircraft (BURPG, 2024). Schmidt et al. (2015) use a cold gas jet thruster to control the attitude aiming to be used in a vacuum condition and Iwaki et al. (2023) have demonstrated the pitch and yaw control to achieve the desired attitude in the rhumb line control.

These systems, however, are mounted at the aft of the rocket and require a lot of internal space to store the different systems next to the rocket motor. An alternative option, which was chosen in the previous project, the *Pathfinder*, in the 2022-23 academic year, involves aerodynamic control by using aerofoils called canards (Youds et al., 2023). These fins positioned mid-section of the rocket adjust their angle of attack in response to changes in orientation.

NASA developed the Boost Guidance System, which uses four canards, operated by two electronic servos with pneumatic support, guided by an LN-200 Inertial Measurement Unit (IMU) (Burth et al., 2023). Attempts to integrate canard control systems into rockets have been explored by several university groups. A notable attempt was by a team from TU Delft (DARE, 2016), who developed a rocket with canard controls effective in the roll axis alone. This modification reportedly mitigated weather cocking and increased the apogee, though it also introduced a downwash effect on the passive fins. This observation influenced the integration of a spin-can design in the Pathfinder (Youds et al., 2023). Additionally, the University of Canterbury stands out as the only team to have launched a rocket equipped with a three-axis active control system (Buchanan et al., 2015).

Whilst a prototype of the *Aptos*, an active attitude control module, had been previously built and field tested in the Pathfinder rocket, it had never been activated during the flight due to insufficient test and verification (Youds et al., 2023). We has conducted to improve an existing active control system by making significant design changes, introducing verification procedures and integrating further data processing methodologies.

⋆ The paper is based on parts of the MEng project, supervised by JK, performed by AP, AM, AD, OM and SB in the 2023-24 academic year at the University of Leeds, Leeds, UK.

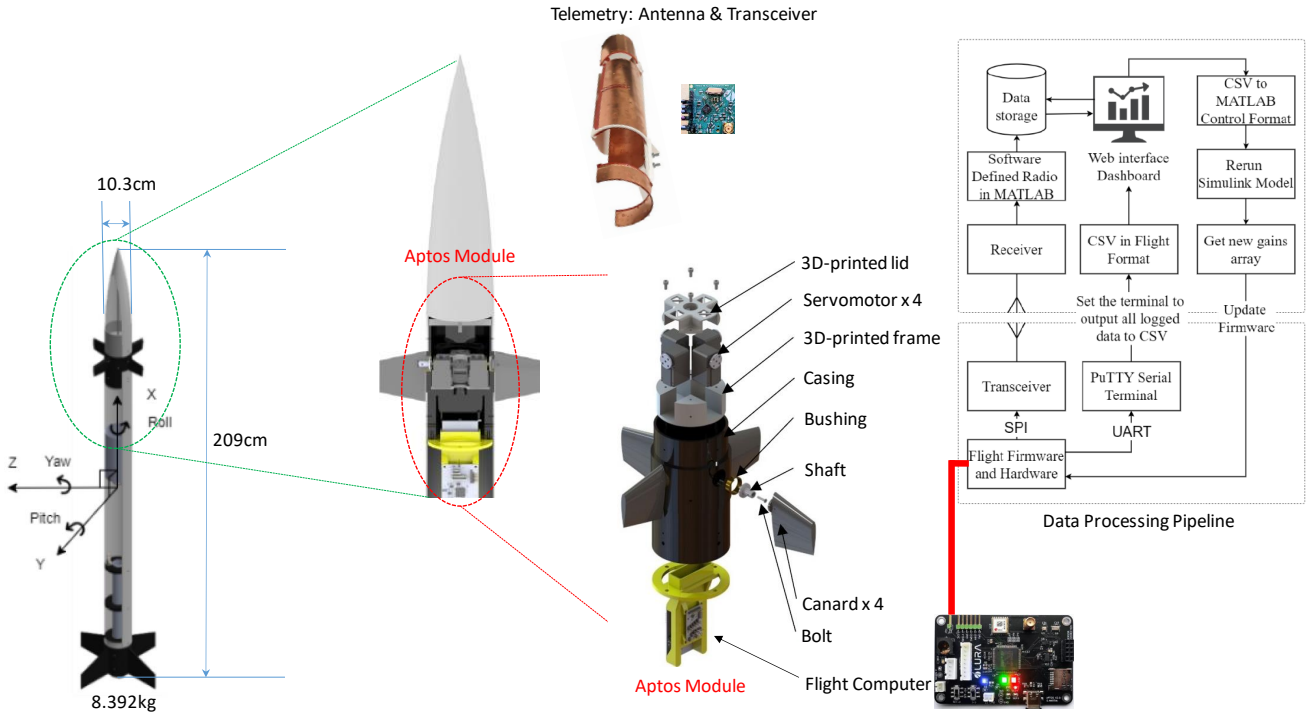

Fig. 1. The Pathfinder sounding rocket, the Aptos module & the data pipeline architecture

The rest of the paper is organised as follows: firstly, the system architecture design is presented; secondly, the verification procedures provides test results; thirdly, the post-flight data are analysed; finally, the conclusions and future works are presented.

2. SYSTEM ARCHITECTURE DESIGN

The Aptos module is positioned below the nose cone at the fore of the rocket as shown in Figure 1. This section presents the summary of design improvements for the Aptos module.

2.1 Mechanical module & canard

The assembly of the Aptos module begins with the installation of four servomotors onto a 3D (3-Dimensional) printed frame. A 3D-printed lid is placed over the servomotors and the entire unit is inserted into a Delrin casing, where bushings are glued. Shafts are attached to the servomotors and secured with bolts. Based on the CFD (Computational Fluid Dynamics) analysis using XFLR5 (2024), among eleven aerofoils from NACA-0010 to NACA-0020, NACA-0016 aerofoil is selected to maximise the lift and minimise the drag. Four canards are mounted onto the shafts and fastened using shear pins. To further safeguard the servomotors from the axial load of the fins, four brass bushings are embedded in the module. These bushings absorb the axial stress, preventing it from impacting the servomotors. They feature a slotted design coupled with a lip that engages with the canards, allowing a controlled motion range of $\pm 15°$ to avoid exceeding the aerofoil stall angle, around 16.5°, estimated by the CFD analysis.

2.2 Avionics & firmware

The flight computer has undergone a complete redesign. The complete system is brought onto a PCB (Printed Circuit Board) with upgraded components. The assembled flight computer, shown in Figure 1, is a four-layer PCB measuring 75×45mm. It is mounted to a PLA (Polylactic Acid) printed bracket on the bottom of the Aptos module using silicone anti-vibration standoffs in the corner mounting holes. The electrical schematics are designed to mitigate the impact of any issues that arise from vibration or component fatigue. Arming switch design incorporates debounce circuits and accounts for fail states to ensure that vibrations or component fatigue do not trigger sudden power-offs. The main parts of the flight computer system are the STM32 MCU (Microcontroller Unit), the IMU, the NAND Flash storage unit and the barometer.

The STM32 uses a SPI (Serial Peripheral Interface) bus to interface with the sensor hardware on the flight computer. Custom drivers have been created to set up and retrieve data from each sensor. The servomotors communicate through single-wire UART (Universal Asynchronous Receiver-Transmitter) to set the servomotor values and command the deflection angles. The LQR (Linear-Quadratic Regulator) controller, designed in Matlab, is translated into C and embedded into the firmware.

2.3 Attitude calculation & control design

The attitude of the rocket is obtained by numerically integrating the quaternion kinematics with the gyroscope-measured angular velocity and the quaternion is transformed into the roll, pitch and yaw angles. The constant bias in the gyroscope is corrected before launch using the gravitational acceleration measurement. As a result, the

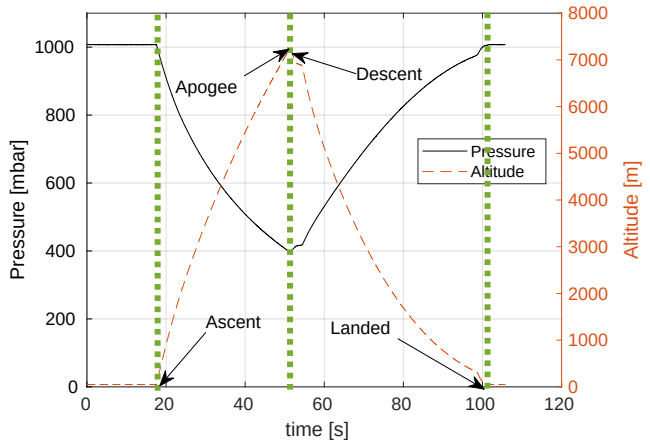

Fig. 2. Flight mode detection test in vacuum chamber

attitude is to drift because of the white noise and the unfixed bias residuals in the angular velocity. The flight time to the maximum altitude is usually less than a few seconds and the effect of drift is tolerable. Due to the lack of verification results, the Kalman filter is not fully adopted in the onboard attitude determination system.

The LQR controller designed in the previous academic year is used, where the coordinate system defined the attitude angles is left-handed, unfortunately, as indicated in Figure 1. A linearised dynamic model is derived, where the state vector includes the roll, pitch, yaw angles and the corresponding angular rates. The cost function weight is set to reduce the pitch and yaw angles (Youds et al., 2023).

2.4 Telemetry

The telemetry system shown in Figure 1 is comprised of a transmission PCB capable of communication with the flight computer board, in addition to a custom antenna design. Receiver software was also built to demodulate and decode the incoming data on the ground. A TI CC1200 transceiver was selected for its small form factor and low cost, whilst providing powerful capabilities. The transmission PCB was capable of 2-way communication, future-proofing the design. The ability to acquire low-cost dielectrically characterised 3D printer filament enabled the production of shaped antennas. It was feasible to develop a curved patch antenna that moulds to the inner tube of the rocket's body. This design allows for space-efficient integration by accommodating the electronics within the antenna itself, while also maximising its size to house a full-wave patch antenna.

2.5 Data Pipeline

A data pipeline sequentially processing data reduces manual handling (Van Alstyne et al., 2016). After each test flight, data from the onboard computer is uploaded to a centralised database for visualisation and analysis. As shown in the diagram in Figure 1, the flight data is loaded into a centralised storage unit using a local MySQL database instance. This database acts as a robust platform for data storage, retrieval, and management (Munappy et al., 2020). The database consists of three tables

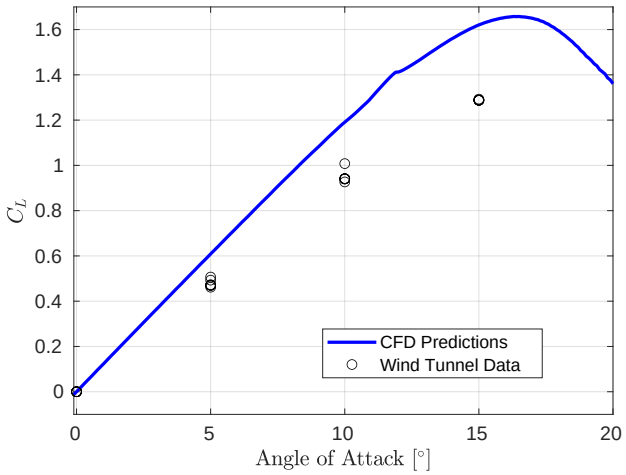

Fig. 3. Lift coefficient (C_L) with respect to angle of attack from CFD and wind tunnel experiment

that store general flight information, sensor readings and controller output. A web-based application has been developed to facilitate data visualisation. Once the flight data is validated, they are exported in Matlab to tune the controller gains with real-world data. This integration promises to simplify and streamline the testing and improvement process of the controller.

3. VERIFICATION PROCEDURE

A systematic verification procedure including the flight mode detection, the wind tunnel and the attitude estimation system tests confirms the integrity of the attitude control system.

3.1 Flight mode detection test

To validate that the flight computer could correctly detect flight stages, the module is placed in a vacuum chamber to simulate the air pressure at higher altitude. The flight computer and battery are placed in the vacuum chamber and the pressure is reduced to -0.6bar from atmospheric pressure. As illustrated in Figure 2, the flight computer interpreted a decrease in pressure as a rocket lift off. After reaching the target pressure, the pump is deactivated and the valve is opened. The flight computer detects the apogee followed by descent. Once at the initial pressure, the landed state is correctly detected.

3.2 Wind tunnel test

The wind tunnel tests were carried out at the ESTACA engineering school in France. A total of four different jigs have been created, each representing a set of two canards with different angles of attack ranging from 0 to 15°. The wind tunnel has a maximum windspeed of 40m/s, and each jig was tested three times. To compare data between simulations and experimental wind tunnel results, the Mach number in the CFD software was also set to 0.121. The lift coefficients from the CFD are higher than the experimental data as shown in Figure 3. These coefficient differences could be caused mainly by the print imperfections of the canards.

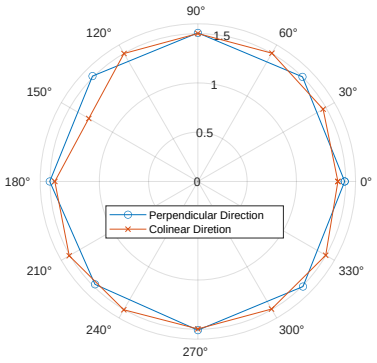

Fig. 4. Telemetry antenna directional power performance

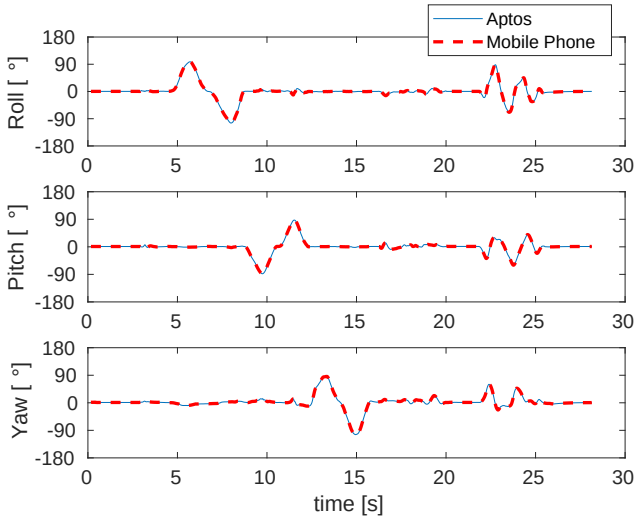

Fig. 5. Aptos flight computer attitude estimation comparison with the mobile device: note that the yaw data of the mobile phone is multiplied by -1 to align the z-axes

3.3 Telemetry test

The telemetry PCB is manufactured and tested, supplying adequately stable voltages, and filtering the output signal at the right frequency without significant reflections. The custom antenna design was effective, as full characterisation demonstrated similar gains and better directional performance than an off-the-shelf helical antenna as shown in Figure 4. The receiver shows reliable frequency tracking when the signal-to-noise ratio is greater than 1.5.

3.4 Attitude estimation test

To assess the performance of the flight computer attitude estimation system, the Aptos was mounted on a DJI Phantom 4 Pro drone to compare flight computer data against the data gathered from the drone. The barometer data of the Aptos shows a large drop in pressure when the drone takes off. This would be the effect of the propeller wash caused by the drone impacting the exposed barometer. Additionally, discrepancies in the orientation data were traced back to motor vibrations.

Alternative tests were conducted in which the flight computer was fixed to a mobile device. Both the flight computer and the phone axes (while the $+z$ axis of the Aptos

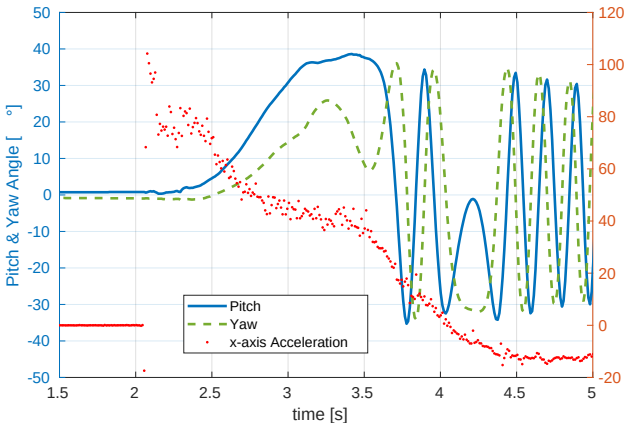

Fig. 6. Flight Record: Pitch and yaw angles and the acceleration in the rocket x-axis

is aligned with the $-z$ axis of the mobile device because of the left-handed coordinate system of the Aptos) were aligned and set to record gyroscope, orientation, and accelerometer data. The roll, pitch and yaw angles in Figure 5 show good agreements between them, where the mean error and the standard deviation of the difference between them are less than 0.51 and 0.3 arcseconds, respectively, for all three attitude angles.

4. LAUNCH & POST-FLIGHT DATA ANALYSIS

The Aptos module is assembled and integrated within the Pathfinder rocket. Using a J570W-14A motor (Wizard Rockets Ltd, 2024), it was launched with the active control enabled to an apogee of 354m. Figure 6 shows the x-axis acceleration and the pitch & yaw angles. There is a slow increase of the attitude angles up to 3.5s. The counteraction canard drove the rocket to point in the opposite direction around at 3.7s. The oscillation keeps repeating as shown in the four snapshots in Figure 7 and the captured video available in (LURA, 2024).

The controller is active when the vertical velocity of the rocket is above 30m/s. Figure 8 shows the four canards started to act at 2.07s. As the rocket separates from the launch pad and increases in velocity, the canards perform correcting movement, reaching the full extent of their operational angle range, $\pm 15°$. As the Aptos module has never been flown with active control enabled before, we reduced the control gains to minimise aggressive control actions and, contrary to the intention, the accumulated error at the beginning caused the controller to command the canards with full deflection after three seconds. The Aptos module, however, was able to keep the flight path in the bounded region, as shown in Figure 9, where the unit vector towards the rocket nose cone projects on the horizontal surface of the ground.

An issue identified in the control design is in the use of OpenRocket simulation to tune the control gains. Figure 10 shows that while OpenRocket simulated an apogee of 462m, the flight reached 354m. It indicates a significant amount of modelling discrepancies. Some of the altitude loss can be linked to the variable deflection of the canards. However, a similar altitude discrepancy of 76m was also noted in the previous year's flights, which were conducted

Fig. 7. Flight Record: Launch Snapshots. The full video is available in (LURA, 2024).

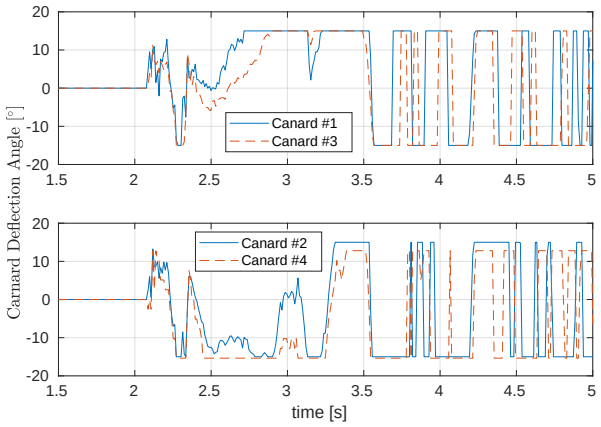

Fig. 8. Flight Record: Canard deflection angles

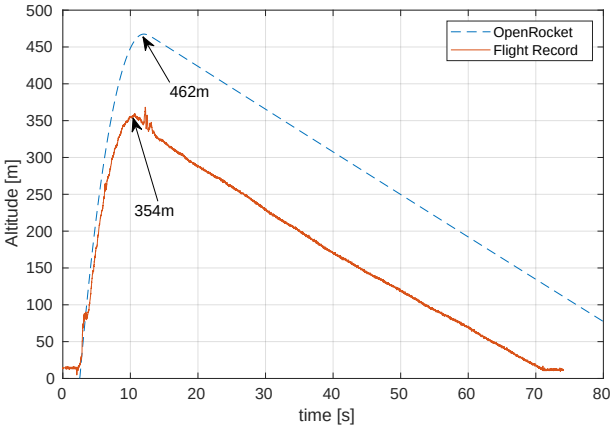

Fig. 10. Altitude comparison: flight data vs. OpenRocket Simulation

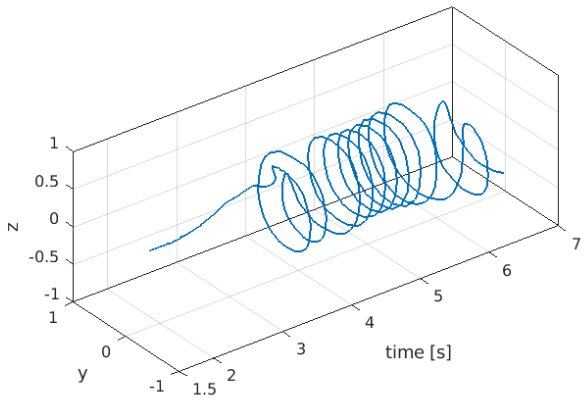

Fig. 9. Flight Record: The trace of the Rocket nose pointing unit vector is projected on the horizontal surface.

with the canards locked at the 0°. This suggests that another variable component, the spincan, likely contributed to the losses. The rotational motion introduced by the spincan is not accounted for in the simulations, highlighting a gap in the modelling process. The ability for the fins to spin freely was important to reduce canard control flow opposition (Silton and Fresconi, 2015). It, however, may induce additional drag by generating turbulent airflow or unwanted horizontal forces.

After the Pathfinder rocket landed and was recovered, the canards were confirmed to be in their neutral position, undamaged, and with the shear pins intact. This could be caused by a softer landing than expected. The ground hit velocity was 5.27m/s, softer than the 5.67m/s predicted by OpenRocket, partly because it landed on top of crop fields, which could have absorbed some of the force.

In the post-flight evaluation, the system pipeline's throughput was quantified at approximately 0.622 MB per minute, which includes the duration of data retrieval from the flight hardware to its eventual ingestion into the database. The primary bottleneck of the system was the NAND Flash's reading speed, which took 92% of the entire pipeline duration. In a future firmware version, the data reading procedure would benefit from further improvement. During the test launch, the data acquisition system used about 2.359Mb of storage. Given the modest storage requirements, it is anticipated that the database could ac-

commodate data from multiple future flights, even with substantial increases in data acquisition rates.

5. CONCLUSIONS & FUTURE WORKS

The Pathfinder has successfully completed the flight with the Aptos active control system and has shown promising results in maintaining the desired flight path. Valuable antenna data was collected and the transmission system survived the flight without breaking. The mechanical transmission system was successfully designed and tested using both aerodynamic simulations and physical tests in the wind tunnel. Custom flight computer and Telemetry PCBs were developed, manufactured and programmed. A custom antenna has also been developed to transmit data to the ground. To allow data to be fed back into the controller, a data storage solution and visualisation tools were implemented.

Areas of the Aptos module which could benefit from further development have been identified as follows: firstly, identifying the major sources of altitude loss; secondly, developing an accurate attitude estimation algorithm and fine-tuning the controller gains or introducing an advanced controller; thirdly, introducing additional sensors such as GNSS and humidity to understand the full details of dynamics; fourthly, improving the telemetry reliability; and finally, improving the visualisation tools to enhance the post-flight analysis.

The lessons learned from the project are as follows:

- Emphasise the importance of consistent coordinate system definition at the beginning of the project
- Test methods need to be carefully designed in terms of the sensor characteristics such as temperature, vibration, pressure and turbulence.
- A week-long short course on the Kalman filters and attitude kinematics is required at the beginning of the project. See Kim (2022), for example.

ACKNOWLEDGEMENTS

We would like to acknowledge the financial support received from the School of Mechanical Engineering, University of Leeds. We are deeply grateful to the industrial advisor of the project, Theo Gwynn of the Airbus Aerospace & Defence, for his guidance and support throughout this project.

Contributions: AP developed the flight firmware, the data processing pipeline and the visualisation; AM developed the telemetry; AD designed the mechanical and aerodynamic parts of the canard system; OM developed the flight computer, firmware & attitude estimation verification; SB designed a single-axis Kalman filter; and JK supervised the project. The paper is written based on the students' final reports submitted to the University of Leeds in the 2023-24 academic year.

REFERENCES

Box, S., Bishop, C.M., and Hunt, H. (2011). Stochastic six-degree-of-freedom flight simulator for passively controlled high-power rockets. *Journal of Aerospace Engineering*, 24(1), 31–45.

Buchanan, G., Wright, D., Hann, C., Bryson, H., Snowdon, M., Rao, A., Slee, A., Sültrop, H.P., Jochle-Rings, B., Barker, Z., McKinstry, A., Meffan, C., Xian, G., Mitchell, R., and Chen, X. (2015). The development of rocketry capability in new zealand—world record rocket and first of its kind rocketry course. *Aerospace*, 2(1), 91–117. doi:10.3390/aerospace2010091.

BURPG (2024). Astro–burpg. URL `https://burpg.org/astro`. Accessed 31-05-2024.

Burth, R.H., Cathell, P.G., Edwards, D.B., Ghalib, A.H., Gsell, J.C., Hales, H.C., Haugh, H.C., and Tibbetts, B.R. (2023). Nasa sounding rockets user handbook. Technical report, NASA.

Candidato, R., Vallini, L., and Bach, C. (2014). Static and dynamic analysis of the aerodynamic stability and trajectory simulation of a student sounding rocket. *Univ. of Pisa aerospace engr. Master's Thesis*, 23–24.

DARE (2016). Advanced control team - Delft. URL `https://dare.tudelft.nl/projects/act/`. Accessed 03-06-2024.

Hervas, J.R. and Reyhanoglu, M. (2014). Thrust-vector control of a three-axis stabilized upper-stage rocket with fuel slosh dynamics. *Acta Astronautica*, 98, 120–127.

Iwaki, T., Yamamoto, T., Nonaka, S., Ogita, T., and Sakoda, Y. (2023). Radio guidance command design for target angle correction of sounding rocket s-520-rd1. In *62nd Annual Conference of the Society of Instrument and Control Engineers (SICE)*, 632–637.

Kim, J. (2022). *Dynamic System Modeling and Analysis with MATLAB and Python: For Control Engineers*. IEEE Press Series on Control Systems Theory and Applications. Wiley-IEEE Press.

LURA (2024). Aptos - LURA. URL `https://leedsrocketry.co.uk/projects/aptos`. accessed 06-06-2024.

Munappy, A.R., Bosch, J., and Olsson, H.H. (2020). Data pipeline management in practice: Challenges and opportunities. In *Product-Focused Software Process Improvement: 21st Int. Conf., PROFES 2020, Turin, Italy, Nov. 25–27, 2020, Proceedings 21*, 168–184. Springer.

Schmidt, E.S., Louke, J., Amell, K., Hickman, J., and Wiles, B. (2015). Development of a low-cost, open hardware attitude control system for high powered rockets. In *AIAA SPACE 2015 Conference and Exposition*. doi: 10.2514/6.2015-4623.

Seibert, G. and Battrick, B.T. (2006). *The history of sounding rockets and their contribution to European space research*. ESA Publications division Noordwijk.

Silton, S.I. and Fresconi, F. (2015). Effect of canard interactions on aerodynamic performance of a fin-stabilized projectile. *J. of Spacecraft & Rockets*, 52(5), 1430–1442.

Van Alstyne, M.W., Parker, G.G., and Choudary, S.P. (2016). Pipelines, platforms, and the new rules of strategy. *Harvard business review*, 94(4), 54–62.

Wizard Rockets Ltd (2024). J570W-14A 38/1080 RMS-PLUS. URL `https://wizardrockets.co.uk/product/j570w-14a-38-1080-rms-plus`. Accessed 06-06-2024.

XFLR5 (2024). xflr5. URL `http://www.xflr5.tech`. Accessed 03-06-2024.

Youds, T., Cradock, B., Devlin, L., Whittaker, J., and Daney de Marcillac, J. (2023). The pathfinder. URL `https://www.youtube.com/watch?v=i7Es2SUi1Qo`. Accessed 30-05-2024.